Th SBT5 08

Downsampling Plus Interpolation for Wavefield Reconstruction by Reverse Propagation

P. Yang* (Universite Grenoble Alpes), R. Brossier (University Grenoble Alpes) & J. Virieux (University Grenoble Alpes)

SUMMARY

In reverse time migration and full waveform inversion applications, one need to access both source and receivers wavefield simultaneously, which is computationally and memory intensive. Due to slow disk reading with huge volume of data, computation-based wavefield reconstruction methods such as checkpointing strategy and wavefield reconstruction by reverse propagation are preferred to achieve efficient implementation in this key step. Compared with checkpointing, reverse propagation is usually more efficient while suffering a stringent memory bottleneck for 3D large scale imaging applications.

In this study, we show that the heavy boundary storage can be dramatically reduced up to one or two order of magnitude, based on the temporal sampling determined by Nyquist principle, rather than the more restrictive relation from the Courant-Friedrichs-Lewy condition. We present three boundary interpolation techniques, namely the discrete Fourier transform interpolation, the Kaiser windowed sinc interpolation and Lagrange polynomial interpolation. The three interpolation methods, in conjunction with different computational efficiency depending on the global (Fourier) basis or local (windowed sinc and polynomial) basis, allow us to accurately reconstruct the boundary elements without significant loss of information, making the in-core memory saving of the boundaries practically feasible in 3D large scale imaging applications.

Introduction

Many seismic imaging and inversion techniques such as reverse time migration (RTM) and full waveform inversion (FWI) are usually computationally and memory intensive. For 3D implementation of such techniques, one significant issue is the imaging-condition of RTM and the gradient-building step of FWI: both of them require to access the forward wavefield backward in time while computing the adjoint/receiver wavefield. Three main strategies can be used to perform this step: (1) reading the stored forward wavefield from disk involving significant I/O's, (2) remodeling the forward wavefield using checkpoints from stored state to needed state (Griewank and Walther, 2000; Symes, 2007; Anderson et al., 2012) or (3) inferring the forward field backward in time from the final snapshots and the stored boundaries via reverse propagation assuming a reversible wave equation (Clapp, 2008; Dussaud et al., 2008; Brossier et al., 2014). Among these techniques, wavefield reconstruction by reverse propagation appears to be quite efficient approach, however, suffering a stringent memory bottleneck for 3D large scale imaging applications.

Wavefield reconstruction by reverse propagation

The main idea of wavefield reconstruction by reverse propagation is to compute the forward wavefield twice: once in forward time during which the boundary values are stored in core-memory (and disk if required) until the final time-step. Then, during the computation of the adjoint/receiver field, the forward field is synchronously recomputed backward in time from the final snapshots, as initial condition, and the saved boundary condition, acting as Dirichlet boundary condition at each time-step (Clapp, 2008; Dussaud et al., 2008; Brossier et al., 2014).

This technique involves to compute the forward field only twice, assuming a reversible wave equation and stable modeling tool, when applied backward in time. The memory bottleneck is associated to the boundary saving. For cubic 3D model of size $n \times n \times n$ and considering N time-steps, the memory requirement scales to $O(a\, n^2 N)$, where a is a constant depending on the number of faces to be stored and length of the numerical stencil, which make the method generally possible. The aim of this study is to show that a downsampling plus interpolation can be applied to significantly reduce the constant a without loss of accuracy, making the approach feasible for even larger problems.

Time-step: from CFL to Nyquist

When discretizing the partial differential equation of time-domain wave-equation using explicit numerical methods, we usually end-up with a Courant-Friedrichs-Lewy (CFL) stability condition such as

$$\Delta t \leq \frac{\Delta x}{v_{\max}} c \tag{1}$$

where Δt and Δx are the temporal and spatial interval after discretization; $v_{\max}$ is the maximum velocity; c is a constant depending on the numerical scheme used. For any numerical method, we can also define d as the number of points per wavelength to be used to reach accurate enough solution. We end up with

$$\Delta x = \frac{\lambda_{\min}}{d} = \frac{v_{\min}}{d\, f_{\max}} \qquad \Rightarrow \quad \Delta t \leq \frac{c\, \Delta x}{v_{\max}} = \frac{c\, v_{\min}}{d\, v_{\max}\, f_{\max}}. \tag{2}$$

Nyquist theorem states that a signal can sampled without loss as long as the sampling frequency is no less than twice of the maximum frequency of the original signal:

$$f_s \geq 2 f_{\max} \quad \Rightarrow \quad \Delta t \leq \frac{0.5}{f_{\max}}. \tag{3}$$

The CFL and Nyquist are therefore two criteria that drive the choice of the time step Δt, the CFL-one being always more restrictive than Nyquist one.

Boundary value saving: relaxing the memory bottleneck thanks to Nyquist

While the numerical simulations done both forward and backward in time have to satisfy the CFL stability limit, as well as the knowledge of the boundary values acting as Dirichlet conditions, the storage of the boundary values could be downsampled up to Nyquist. Assuming an interpolation technique can be implemented to synthesis the missing boundary values from the downsampled version of the signal, a significant memory saving can be achieved. This saving follows the ratio r between time-step from

Nyquist and the one from CFL

$$r = \left(\frac{0.5}{f_{\max}}\right) / \left(\frac{c\, v_{\min}}{d\, v_{\max}\, f_{\max}}\right) = \frac{0.5\, d\, v_{\max}}{c\, v_{\min}}. \tag{4}$$

For illustration, if we consider a 3D case with 4^{th} order staggered-FD scheme in space and 2^{nd} order FD leap-frog scheme in time, we have $c \approx 0.49487$ and $d \approx 5$ points per wavelength. That leads memory reduction of factor 5 in homogeneous acoustic media, factor 10 in heterogeneous acoustic media with $v_{\max} = 2 \times v_{\min}$ and factor 50 in heterogeneous elastic media with $v_{P\max} = 10 \times v_{S\min}$.

Boundary interpolation methods

In this study, we present three boundary interpolation techniques, namely the *discrete Fourier transform (DFT) interpolation*, *Kaiser windowed sinc interpolation* and *Lagrange polynomial interpolation*. Assume the boundary are decimated during N steps forward simulation with factor $r = N/M$. The reconstruction via DFT interpolation for wavefield boundaries $u(\mathbf{x},t)$ utilizing the global Fourier basis can be implemented on the fly by folding steps

$$\tilde{u}(\mathbf{x},k) = \sum_{m=0}^{M-1} u(\mathbf{x},t'_m) e^{-j\frac{2\pi k}{M}m} = \sum_{m=0}^{M-1} u(\mathbf{x},t_{mr}) e^{-j\frac{2\pi k}{M}m}, k = 0,1,\ldots,\lfloor M/2 \rfloor + 1 \tag{5}$$

involving $O(N^2/r^2)$ flops of computation in the forward simulation and unfolding steps

$$u(\mathbf{x},t_n) = \begin{cases} \frac{1}{M}\left(\tilde{u}(\mathbf{x},0) + 2\Re\{\sum_{k=1}^{\frac{M-1}{2}} \tilde{u}(\mathbf{x},k) e^{j\frac{2\pi k n}{N}}\}\right) & \text{for odd } M \\ \frac{1}{M}\left(\tilde{u}(\mathbf{x},0) + 2\Re\{\sum_{k=1}^{\frac{M}{2}-1} \tilde{u}(\mathbf{x},k) e^{j\frac{2\pi k n}{N}}\} + \tilde{u}(\mathbf{x},\frac{M}{2})\cos(\frac{\pi n}{r})\right) & \text{for even } M \end{cases} \tag{6}$$

involving $O(N^2/r)$ flops of computation in backward reconstruction. Compared with the DFT interpolation, the boundary reconstruction methods using Kaiser windowed sinc interpolation and Lagrange polynomial interpolation are much more efficient because the decimated boundary values are stored directly without any computation and the missing values are interpolated with $O(N)$ flops according to local basis functions (the Lagrange polynomial $\ell(t_n)$ or sinc function $h(t_n)$ modulated by Kaiser window $w(t_n)$ within the support W)

$$u(\mathbf{x},t_n) = \sum_{i\in W} u(\mathbf{x},t'_i)\ell_i(t_n) \quad \text{or} \quad u(\mathbf{x},t_n) = \sum_{i\in W} u(\mathbf{x},t'_i) w(t_n - t'_i) h(t_n - t'_i). \tag{7}$$

They are excellent alternatives to DFT interpolation algorithm, to alleviate the computational complexity without significant sacrifice of wavefield reconstruction quality. These interpolation methods allow us to greatly decimate the boundary without significant loss of information, and accurately reconstruct the boundary elements in between the samples, making the in-core memory saving of the boundaries practically feasible in 3D large scale imaging applications.

In order to illustrate the achievable memory saving, let us consider a 3D model of size $nx \times ny \times nz$. Allowing for minimum boundary saving burden using $2J$-th order staggered grid finite difference modeling for N time steps, $2J-1$ layers for saving single state variable of the cube are required (Yang et al., 2014a,b; Nguyen and McMechan, 2015). Thus one time step requires a storage along the boundary of $S = 2(2J-1)(nx \times ny + nx \times nz + ny \times nz)$.

Assuming single precision (one real value needs 4 bytes) in the computation of wave propagation, the original time domain wavefield reconstruction scheme needs $N \times S \times 4$(Bytes) memory consumption without any additional computational efforts because the saved boundaries are directly stuffed in their corresponding locations in backward reconstruction. The proposed DFT interpolation algorithm for wavefield reconstruction with a downsampling factor r involves $\frac{N}{r} \times S \times \frac{1}{2} \times 8$(Bytes) to store the Fourier coefficients (one complex-valued coefficient needs 8 bytes while only positive frequencies are saved) of the boundary elements during folding procedure. The local-based Kaiser windowed sinc interpolation and Lagrange polynomial requires the same amount of memory for the same r value, as real value of time-domain signal are stored instead of complex-value Fourier coefficient for real frequencies only.

Considering again an example with staggered-grid FD $O(\Delta x^4, \Delta t^2)$ and $nx = ny = nz = 300$, $N = 4000$,

$2J = 4$, the original wavefield reconstruction scheme using boundaries stored at every time step would leads to a memory requirement of $N\ S\ 4/1024^3 = 24.14$(GB). For a realistic acoustic model with $v_{\max}/v_{\min} \geq 2$, the downsampling factor will be larger than 10 and the memory consumption drops to $24.14/r < 2.42$(GB). In elastic media, the velocity contrast would be much higher in realistic media: $v_{\max}/v_{\min} > 10$. For the same set-up, the memory consumption drops lower than 0.48(GB). The proposed method is therefore quite valuable when the velocity model becomes more complex with high velocity contrasts.

Numerical example in 2D with Marmousi

To demonstrate the validity of the proposed methods, we run our downsampling plus interpolation algorithm on a resampled version of the 2D Marmousi model with $nz \times nx = 251 \times 767$, a grid spacing $\Delta x = \Delta z = 12m$ and $N = 3600$ time steps using the temporal sampling $\Delta t = 0.001s$. Due to the large velocity variation in the Marmousi model ($v_{\min} = 1500m/s$, $v_{\max} = 5500m/s$), a significant downsampling ratio $r = 15$ is used. In order to assess the accuracy of our method, the monitoring of two snapshots at time-steps $n = 400$ and $n = 1200$ are displayed in Figure 1. Figures 1a and b show the forward time snapshots. Panels (c-d), (e-f) and (g-h) show the error during the simulation backward in time for the three interpolation methods : DFT, Kaiser windowed sinc interpolation and Lagrange polynomial interpolation respectively. Note that the error plots are two orders of magnitude smaller that the forward simulated wavefield panels (a-b). Thanks to the global interpolation base, DFT provides better accuracy on the snapshots. The same order of error level is still reached with the two other methods.

For a more quantitative view of the error, we also extract a trace at the grid point (100,100). The results obtained from DFT-based reconstruction, Kaiser sinc interpolation-based reconstruction (with 8-points window) and the Lagrange polynomial-based reconstruction (with polynomial of order 7) are shown in Figure 2a-c. The errors between the forward simulated trace and backward reconstructed traces from the three methods are of similar accuracy, and quite acceptable for imaging purposes, proving the benefit of such approach for RTM and FWI.

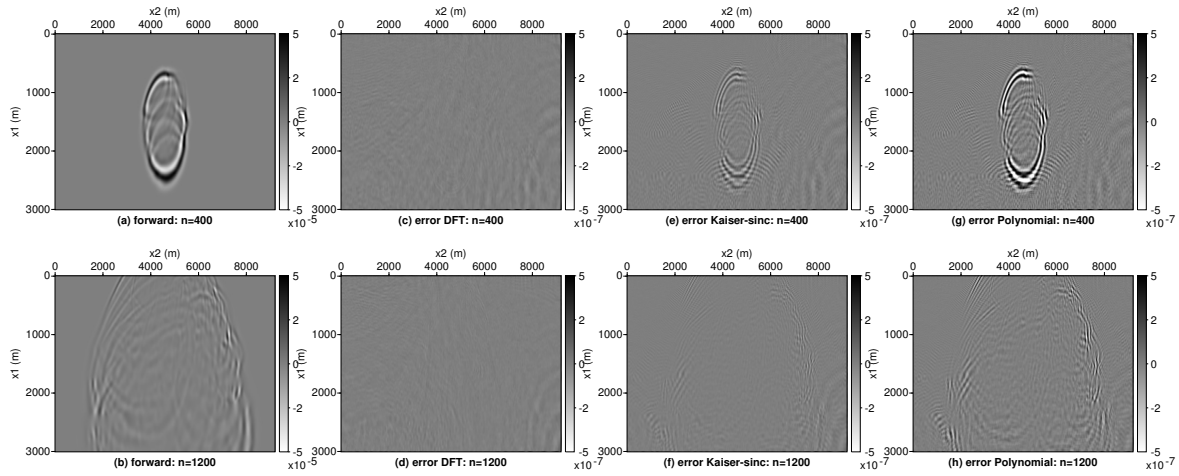

Figure 1 *(a,b) With the downsampling rate $r = 15$, two snapshots are recorded during forward modeling in Marmousi model. Good reconstruction performance is demonstrated using (c,d) DFT-based boundary interpolation, (e,f) Kaiser windowed sinc interpolation and (g,h) Lagrange polynomial interpolation. Note that the amplitude of the error panels in (c–h) are 2-3 orders of magnitude smaller compared with the forward simulated wavefield in (a,b).*

Conclusion

This study shows that the wavefield reconstruction by reverse propagation used in RTM and FWI appears quite appealing and promising, in particular when combined with the proposed downsampling plus interpolation method. We have investigated three interpolation methods, namely the DFT, the Kaiser windowed sinc and Lagrange polynomial interpolation methods. The three methods allow the same amount of memory saving in the downsampling step. The DFT interpolation provides better accuracy of the reconstructed wavefield, than Kaiser windowed sinc and Lagrange polynomial, but the three are able

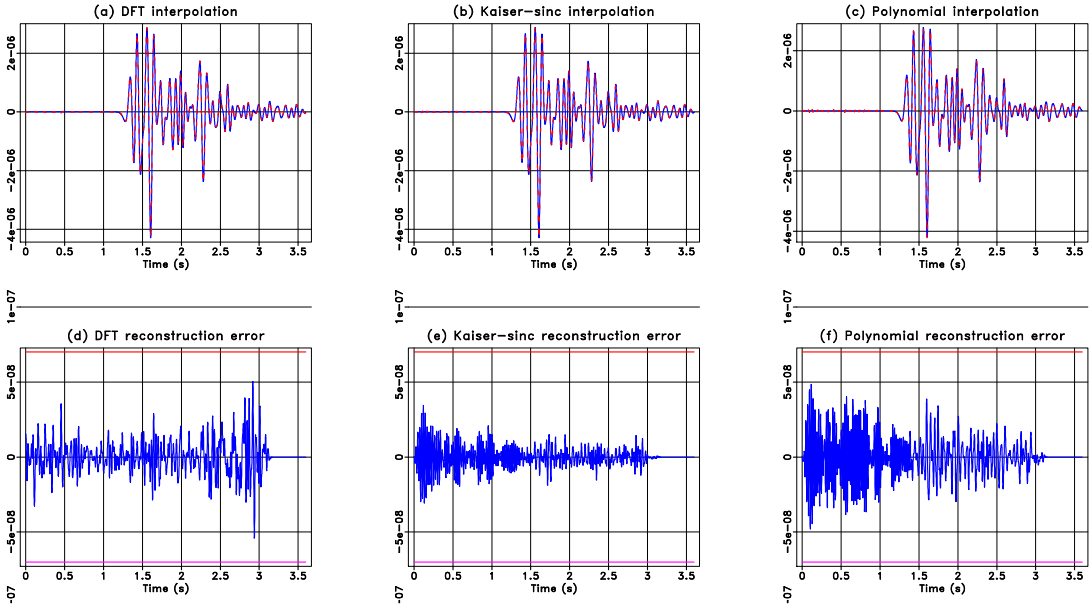

Figure 2 *Trace comparison of wavefield reconstruction methods for the Marmousi model at location (100,100). Top line (a–c): In each panel the interpolated signals (solid) exactly match the raw trace (dash) using different method; Bottom line (d–f): The corresponding error traces obtained by subtracting the interpolated signal with the true one. Note that the amplitude of the errors are several order of magnitude smaller than the original signal.*

to reach acceptable error level for imaging purposes. The global-base DFT approach is however more computationally intensive as it scales to $O(N^2)$ for each stored value and N time-steps simulation during the folding and unfolding steps. The local-base approaches, the Kaiser windowed sinc and Lagrange polynomial interpolation methods, scales to $O(N)$ for each stored value during the unfolding step while being free of extra-computation during the forward simulation. In a companion study (Yang et al., 2016), we show how this downsampling plus interpolation for wavefield reconstruction by reverse propagation can also be used in combination to checkpoint in viscous media for which the wave-equation is not reversible.

Acknowledgments

We thank Stephane Operto and Ludovic Metivier for stimulating discussions. This study was partially funded by the SEISCOPE consortium (*http://seiscope2.osug.fr*), sponsored by BP, CGG, CHEVRON, EXXON-MOBIL, JGI, PETROBRAS, SAUDI ARAMCO, SCHLUMBERGER, SHELL, SINOPEC, STATOIL, TOTAL and WOODSIDE.

References

Anderson, J.E., Tan, L. and Wang, D. [2012] Time-reversal checkpointing methods for RTM and FWI. *Geophysics*, **77**, S93–S103.

Brossier, R., Pajot, B., Combe, L., Operto, S., Métivier, L. and Virieux, J. [2014] Time and frequency-domain FWI implementations based on time solver: analysis of computational complexities. In: *Expanded Abstracts, 76th Annual EAGE Meeting (Amsterdam)*.

Clapp, R. [2008] Reverse time migration: Saving the boundaries. Tech. Rep. SEP-136, Stanford Exploration Project.

Dussaud, E., Symes, W.W., Williamson, P., Lemaistre, L., Singer, P., Denel, B. and Cherrett, A. [2008] Computational strategies for reverse-time migration. In: *SEG technical program expanded abstracts 2008*, Society of Exploration Geophysicists, 2267–2271.

Griewank, A. and Walther, A. [2000] Algorithm 799: revolve: an implementation of checkpointing for the reverse or adjoint mode of computational differentiation. *ACM Transactions on Mathematical Software (TOMS)*, **26**(1), 19–45.

Nguyen, B.D. and McMechan, G.A. [2015] Five ways to avoid storing source wavefield snapshots in 2D elastic prestack reverse time migration. *Geophysics*, **80**(1), S1–S18.

Symes, W.W. [2007] Reverse time migration with optimal checkpointing. *Geophysics*, **72**(5), SM213–SM221.

Yang, P., Brossier, R., Métivier, L. and Virieux, J. [2016] Checkpointing-assisted Reverse Forward Simulation: an optimal recomputation method for FWI and RTM. In: *Expanded Abstracts, 78th Annual EAGE Meeting (Vienna)*.

Yang, P., Gao, J. and Wang, B. [2014a] RTM using effective boundary saving: A staggered grid GPU implementation. *Computers & Geosciences*, **68**, 64–72.

Yang, P., Wang, B. and Gao, J. [2014b] Using the Effective Boundary Saving Strategy in GPU-based RTM Programming. In: *SEG technical program expanded abstracts 2014*. Society of Exploration Geophysicists.